

## Application of Silica/polyacrylamide nanocomposite as Anticorrosive layer for Steel

Gamal A. El-Mahdy<sup>1,2</sup>, Ayman M. Atta<sup>1,3</sup>, Hamad A. Al-Lohedan<sup>1</sup>, Ahmed M. Tawfik<sup>4,5</sup>,  
Ahmed A. Abdel -Khalek<sup>5</sup>

<sup>1</sup> Surfactant Research Chair, Department of Chemistry, College of Science, King Saud University, Riyadh 11451, Saudi Arabia.

<sup>2</sup> Chemistry department, Faculty of Science, Helwan University, Helwan 11795, Egypt.

<sup>3</sup> Petroleum application department, Egyptian petroleum research institute, Nasr city 11727, Cairo, Egypt.

<sup>4</sup> College of Science, King Saud University, Riyadh, Saudi Arabia

<sup>5</sup> Chemistry department, Faculty of Science, Beni Suef University, Beni Suef, Egypt.

\*E-mail: [gamalmah2000@yahoo.com](mailto:gamalmah2000@yahoo.com)

*Received:* 9 September 2014 / *Accepted:* 28 October 2014 / *Published:* 17 November 2014

---

This work is aimed at developing and investigating silane based organic–inorganic hybrid polyacrylamide nanocomposite possessing unique properties, which can be used to improve the corrosion inhibition of steel subjected to corrosion. The nanocomposite was prepared using dispersion radical polymerization technique. Silica/polyacrylamide nanocomposite with various concentrations have been tested as potential inhibitor against corrosion of steel in 1 M HCl solution using electrochemical techniques. The nanocomposite behave as mixed type inhibitor and forms an inhibitive layer on the metal surface. The inhibition efficiency increased with increase in concentration of silica/polyacrylamide nanocomposite. It was found that the silica/polyacrylamide nanocomposite inhibited the acid induced corrosion of steel better than experienced by silica alone.

---

**Keywords:** silicon, polyacrylamide, corrosion, steel, Polarization, EIS

### 1. INTRODUCTION

Surface modification of inorganic fillers with a polymer shell attracted more attention because the polymer coating alters the interfacial properties of these modified particles [1]. The thermal and the mechanical properties of the hybrid polymers can be improved by the compatibility of the nanoparticles with the polymer matrix. The physical properties of inorganic core of nanoparticle and the surrounding shell organic layer are governed by both the size and shape of the inorganic core. The

surfaces of inorganic materials are functionalized or coated with the polymer chains either through covalent bonding (chemically) or physisorption (physically). Physisorption of polymers can be occurred by absorption of block copolymers with sticky segments or self assembly [2, 3]. The incorporation of silica particles into nanocomposite colloids offers a lot of promising perspectives [4, 5]. Various methods have been developed for preparation of them and they typically involve heterophase polymerization [6-8] (usually resulting in polymer encapsulation of silica nanoparticles), sol-gel process (resulting in coating of polymer colloids with silica), [9-11] with silica), and self-assembly [3]. The nanocomposite particles and the polymer encapsulation of silica nanoparticles are now recognized that these materials can exhibit unusual, even unique, properties [11] which cannot be obtained simply by comixing the polymeric component with the inorganic phase [12, 13]. The silicate nanoparticles (Laponite) was used to form crosslinked composite [14]; the encapsulation of silica in the crosslinked polymers was not reported in the literature.

The pretreatment of metals such as aluminum alloys, mild steel, galvanized steel and stainless steels with silane formulation instead chromatising pretreatment, which is currently being used by the industry, has attracted a considerable industrial interest [15-18]. It is a promising technology for surface modification and corrosion protection of several metallic substrates. The important features of the silane pretreatment is the formation of a very dense self assembled silicon and oxygen rich network – the silane film which forms a physical barrier to the penetration of electrolyte towards the metallic substrate [19]. One major drawback with the application of silane films is the failure to offer an adequate long-term protection due to the presence of cracks, micropores and areas with low cross-link density. This failure facilitates the diffusion of aggressive electrolyte to the coating/substrate interface and is preferential sites for corrosion initiation [19, 20]. Several attempts have been developed to enhance the protective effect of silanes by combining them with other corrosion protection systems such as silica nanoparticles or corrosion inhibitors [19–22]. In this work, hydrophilic silica was dispersed in water and used to prepare nanogel composite based on acrylamide nanogel. The prepared silica hypride nanogel can be used as thin film corrosion protection layer for steel from the corrosive environment such as HCl aqueous solution. The corrosion inhibition efficiency was monitored using electrochemical polarization and impedance measurements.

## 2. EXPERIMENTAL

### 2.1. Materials

Acrylamide, N, N- methylenebisacrylamide, potassium persulfate (KPS), poly(vinyl pyrrolidone) has molecular weight 40000g/mol (PVP), N,N,N',N'-tetramethylethylenediamine (TEMED) were purchased from Aldrich chemical Co. Hydrophilic precipitated silica particle (degree of hydrolysis 100 %) was a gift from Eka Chemicals. The working electrode was steel with the following composition (wt.%): 0.14% C, 0.57% Mn, 0.21% P, 0.15% S, 0.37% Si, 0.06% V, 0.03% Ni, 0.03% Cr and and the balance Fe was used in the study. The surface is ground with different grade emery papers (400, 600, 800, 1000 and 1600 and 2000). The electrode surface was subsequently

cleaned by washing with distilled water, rinsed with acetone and finally washed thoroughly with distilled water for many times and quickly immersed into the test solution. The corrosion tests were performed in 1 M HCl solution in the absence and presence of various concentrations of Silica/polyacrylamide nanocomposite ranging from 50 to 250 ppm.

## 2.2. Preparation of Nanocomposite

The nanocomposite latex was synthesized using free radical copolymerization of styrene and in the presence N, N- methylenebisacrylamide as a crosslinker. Atypical preparation procedure of nanogel is described as follows: In one 100 mL round-bottom flask, 0.125 g of hydrophilic silica and 0.5 g PVP were mixed with 50 mL of ethanol/H<sub>2</sub>O. The solution was stirred at room temperature for 2 h. The flask was purged with nitrogen, and the acrylamide (1 g), MBA (28.3  $\mu$ l) was successively introduced at room temperature under stirring. Finally, 0.0125 g KPS initiator (dissolved in 3ml H<sub>2</sub>O) and 20  $\mu$ l TEMED were added to start polymerization process. The crosslinking copolymerization was carried out at temperature 45 °C for 6 hrs. The nanogel composite was separated by ultracentrifuge at 20000 rpm and washed with ethanol several times.

## 2.3. Characterization

The sizes of the spherical primary silica particles were measured by transmission electron microscopy (TEM) using a JEM-2100F, JEOL, Japan at an acceleration voltage 180 kV. The droplet of dispersed silica was deposited and dried on a carbon coated copper grid (300 mesh).

The surface and interfacial tension measurements between water solution and styrene was measured at 25 °C by means of the pendant drop technique using drop shape analyzer model DSA-100 (Kruss, Germany). Pendant drops were formed on the tip of a Teflon capillary with an outside diameter of 0.1 in. and inside diameter of 0.076 in. The surface and interfacial tension values are the arithmetic means of five experiments. The accuracy of the measurements was  $\pm 0.1$  mN/m. These measurements indicated high degree of accuracy and precision.

## 2.4. Electrochemical measurements

An electrochemical cell with three-electrode configuration consisting of steel as working electrode, a platinum sheet as counter electrode, and saturated calomel electrode (SCE) was used as the reference electrode was used through electrochemical tests. The electrochemical measurements were carried out using an instrument potentiostat (Solartron 1470E system) with Solartron 1455A as frequency response analyzer to perform all polarization and EIS measurements. The experiments were started only after a stable open circuit potential (OCP) was achieved usually within the exposure time of 60 min. A rate of 1 mV/s was used to scan a range of  $\pm 250$  mV with respect to open circuit potential. The EIS experiments were realized in the frequency range from 10 kHz to 0.01 Hz with

perturbation amplitude of 0.005 V peak-to-peak. Data were collected and analysed using CorrView, Corr- Ware, Zplot and ZView software.

### 3. RESULTS AND DISCUSSION

Encapsulation of silica by polyacrylamide has been achieved in dispersion polymerization, with the aid of PVP as stabilizer. The success of encapsulation depends on the hydrophilicity of silica which facilitates the interaction with acrylamide monomer. Solvent H<sub>2</sub>O/ethanol solvent is used to obtain high dispersion of silica nanoparticle. PVP is used as a polymeric stabilizer to achieve

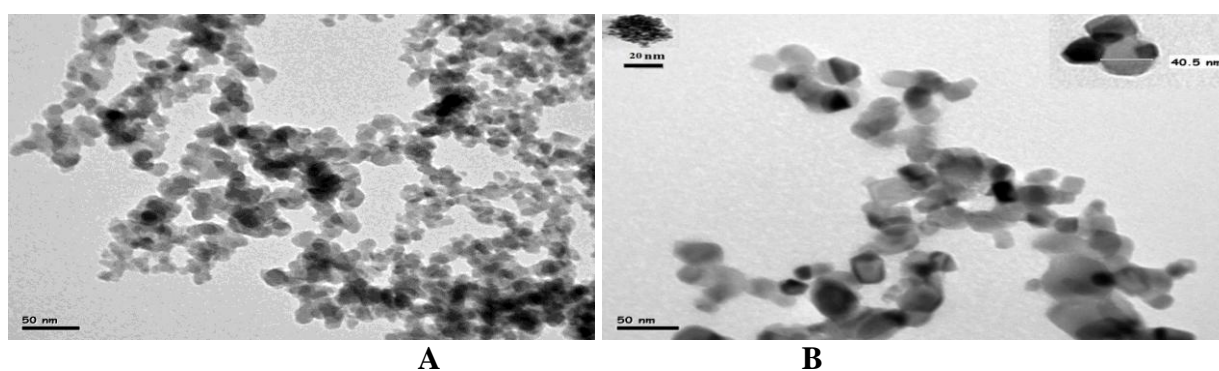


**Figure 1.** TEM micrograph of a) silica and b) silica/polyacrylamide nanocomposite.

TEM image reveals that core shell structure with well defined morphology is successfully prepared. The polyacrylamide completely surround the silica, the particle size was ranged from 35 to 45 nm. It is highly probable that the mechanism of polymerization plays an important role in the final particle sizes and morphology. Indeed, in conventional dispersion polymerization, the particle size is dependent on the solubility of the polymer in the dispersion medium and on the amount or nature of the stabilizer [23]. An excess of stabilizer at any stage of the polymerization can cause further nucleation to occur, while a deficiency of stabilizer leads to particle coalescence. From the dispersant-limited agglomeration theory [23], it is known that the polymer particles result from the agglomeration of much smaller primary particles that are initially unstable. The stabilizer, which is insufficient to cover the total surface area of the primary particles, redistributes onto the reduced surface area of the aggregates and prevents further agglomeration.

EM micrograph contains a dark central zone, a dark outer shell and white circle in between the central zone and outer shell. The dark zones represent the silica nanoparticles while the white surround represents poly(acrylamide) and PVP layer since the inorganic constituents of clay nanoparticles scatter the electron beam than the polymer leading to appearance of dark ones. The TEM micrograph of silica Figure 1a indicated the formation of silica network. The presence of the polyacrylamide nanogel increases the silica dispersion and hindered the formation of the silica network. . The image, Figure 1a, indicated that the silica with an average particle diameter of 20-25 nm was dispersed and

produced networks having particle diameters of 200 nm. The network formation was hindered with the presence of polyacrylamide nanogel more than PVP stabilizer.

The knowledge of surface properties of surface active materials is important in the research and industry. In this respect, the surface tension of water will be measured in absence and presence of silica particle or silica/polyacrylamide to study the adsorption characteristics at interfaces and micellization of the surfactants in bulk solutions. The dynamic surface tension of the silica and silica/polyacrylamide was measured at water/air interface at temperature of 25 °C. The relation between the surface tension of rosin surfactant aqueous solutions with aging time and their concentrations were represented in Figure 2.

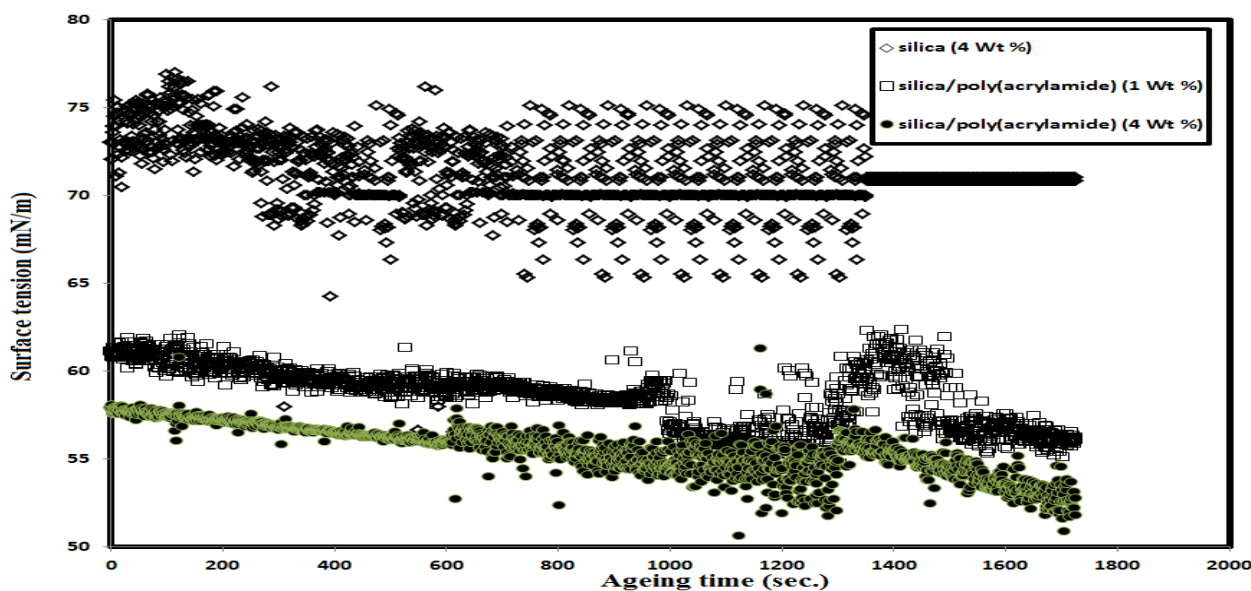


**Figure 2.** Relation between surface tension and ageing time for aqueous solution of silica and silica/polyacrylamide nanocomposite.

The data indicated that, the surface tension of water increased in the presence of silica. Silica/polyacrylamide reduced the surface tension of water from 72 to 50 mN/m. This observation indicated that the formation of silica network in water increased the surface tension as indicated from TEM (figure 1). It has also been suggested that the amide groups of polyacrylamide can be acted as bridges between silica solid particles that facilitating their adsorption at interface. Moreover, small surface micelles are formed owing to hydrophobic association between the polymer backbone. This model indicated that the acrylamide molecules first adsorb as individual molecules through interaction with OH groups of silica, and then associate into hemimicelles. It was reported that the hemimicelles were formed with hydrophobic patches on the surface when the head groups of any surfactants attached to the silica particles and oriented their tail groups toward solution [24]. Further adsorption of the crosslinked polyacrylamide molecules formed second layer of bilayer on silica surfaces [24].

### 3.1 Potentiodynamic polarization

Potentiodynamic polarization curves for steel in 1 M HCl, in absence and presence of silica and silica/polyacrylamide nanocomposite are shown in Figure 3 and 4, respectively. It can be seen from Figures 3-4 that the  $E_{\text{corr}}$  values for steel in 1 M HCl shift slightly toward more negative direction from the uninhibited sample with the addition of silica and silica/polyacrylamide nanocomposite. Both the cathodic and anodic current decrease in presence of silica and silica/polyacrylamide nanocomposite. Figures 3 and 4 apparently show that the cathodic current densities considerably reduce even at low inhibitor concentrations. It can be concluded that the cathodic active sites of the steel may be almost covered by the silica/polyacrylamide nanocomposite. In addition, the inhibition of anodic reaction depends on the inhibitor concentration. Electrochemical parameters namely corrosion current densities ( $i_{\text{corr}}$ ), corrosion potential ( $E_{\text{corr}}$ ), the cathodic Tafel slopes ( $bc$ ), anodic Tafel slopes ( $ba$ ) obtained from the potentiodynamic polarization curves are given in Tables 1 and 2 for silica and silica/polyacrylamide nanocomposite, respectively. The inhibition efficiency IE (%) was computed using the equation [25-27]:

$$\%IE = \frac{i_{\text{corr}} - i_{\text{corr(inh)}}}{i_{\text{corr}}} \quad (1)$$

where  $i_{\text{corr}}$  and  $i_{\text{corr(inh)}}$  are the values of corrosion current density of uninhibited and inhibited specimens, respectively. The inhibition efficiency (IE%) obtained from the potentiodynamic polarization curves are given in Tables 1 and 2 for silica and silica/polyacrylamide nanocomposite, respectively. The reduction in  $i_{\text{corr}}$ , and related IE% pronounces more and more with the increasing silica and silica/polyacrylamide nanocomposite concentration. The increasing inhibition efficiency with increasing inhibitor concentration suggests that this nanocomposite acts by adsorption on the steel surface [28].

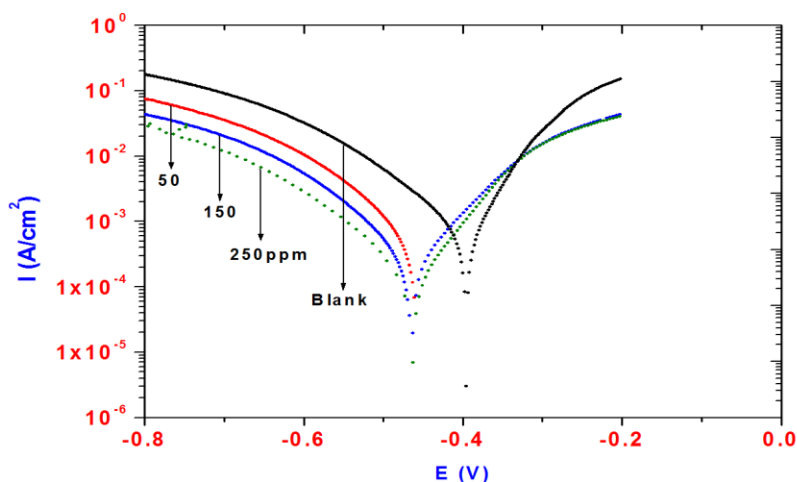


**Figure 3.** Polarization curves for steel in 1M HCl solution containing different concentrations of silica.

The inhibition effect of the inhibitor may be caused by the simple blocking effect, namely the reduction of reaction area on the corroding surface [29–31]. It is expected that, a higher coverage of the inhibitor film on the steel surface forms at higher inhibitor concentrations, which provide better

inhibition efficiency. This means that the inhibitor film behaves as a protective barrier at the steel surface and reduces the corrosion of the steel in the acidic solution. The resistance of steel in the presence of silica and silica/polyacrylamide nanocomposite is higher than that obtained in the absence of inhibitor which, indicates that the adsorption of the inhibitor on the steel surface considerably reduces the corrosion rate of steel even at low inhibitor concentration.

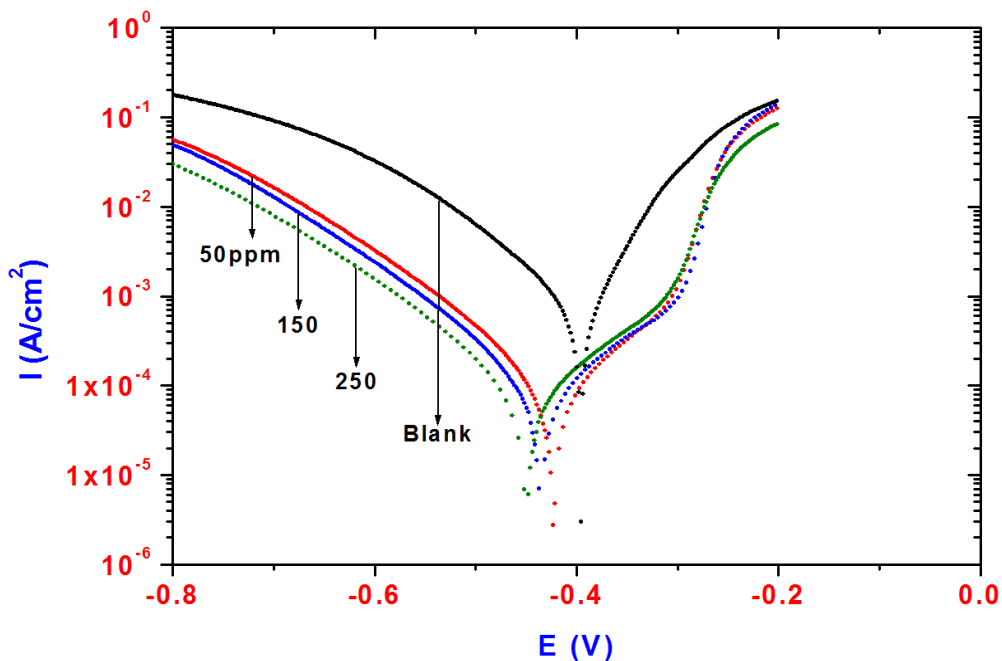


**Figure 4.** Polarization curves for steel in 1M HCl solution containing different concentrations of silica/polyacrylamide nanocomposite.

**Table 1.** Inhibition efficiency values for steel in 1M HCl with different concentrations of silica calculated by Polarization and EIS methods

	Polarization Method					EIS Method		
	Ba (mV)	Bc (mV)	E <sub>corr</sub> (V)	i <sub>corr</sub> , μA/cm <sup>2</sup>	IE%	R <sub>p</sub> , Ohm	Cdl, (μF/cm <sup>2</sup> )	IE%
Blank	69.0	120.0	-0.3955	839	—	1.80	334	—
50ppm	96.8	97.9	-0.4582	445	46.9	3.1	260	41.9
150	92.2	104.5	-0.4643	293	65.7	4.7	180	61.7
250	77.5	105.0	-0.4636	153	81.7	9.0	136	80

**Table 2.** Inhibition efficiency values for steel in 1M HCl with different concentrations of silica/polyacrylamide nanocomposite calculated by Polarization and EIS methods

Polarization Method						EIS Method		
	Ba (mV)	Bc (mV)	E <sub>corr</sub> (V)	i <sub>corr</sub> , μA/cm <sup>2</sup>	IE%	R <sub>p</sub> , Ohm	Cdl (μF/cm <sup>2</sup> )	IE%
Blank	69	120	-0.3955	839	—	1.80	334	—
50ppm	140	113	-0.4352	94	88.79	14.8	118	87.8
150	135	116	-0.4352	83	90.10	15.5	116	88.4
250	97	96	-0.4494	66	92.13	23.0	109	92.1

3.2. Electrochemical impedances spectroscopy measurements (EIS)

Nyquist plots of steel in uninhibited and inhibited acidic solutions (1 MHCl) containing various concentrations of silica and silica/polyacrylamide nanocomposite are given in Figures 5 and 6, respectively. The Nyquist plots contain depressed semi-circles and their size increases with inhibitor concentration, which indicates that the corrosion of steel in 1 M HCl solution is mainly controlled by a charge transfer process [32-34]. The diameter of Nyquist plots increases after adding the inhibitor to the aggressive solution, which clearly shows an enhancement in the corrosion resistance of the metal. The EIS data were fitted to the electrical equivalent circuit in order to model the steel/ solution interface in the absence and presence of the inhibitor [35]. The circuit consists of R<sub>s</sub> the electrolyte resistance, R<sub>ct</sub> is the charge transfer resistance, CPE is Constant Phase Element. The use of a CPE is required for modeling the frequency dispersion generally related to the surface heterogeneity [36]. This can be attributed to the surface heterogeneity due to impurities or dislocations [37], surface roughness, distribution of activity centers, fractal structures, adsorption of inhibitors and formation of porous layers [38–41]. The suggested equivalent circuit model could reasonably represent the charge transfer of steel/ solution interface features related to the corrosion process of steel in acidic solution containing --silica and silica/polyacrylamide nanocomposite. The impedance of CPE was used to replace double layer capacitance (Cdl) for a more accurate fit, which is described as follows [42–44]:

$$Z_{CPE} = Y_0^{-1} (j\omega)^{-n}$$

where Y<sub>0</sub> is a proportional factor, j<sup>2</sup> = -1 is an imaginary number, and ω is the angular frequency (ω= 2πf). If n = 1, the impedance of CPE is identical to that of a capacitor, and in this case Y<sub>0</sub> gives a pure capacitance (C).

The IE% was calculated using the following equation:

$$IE\% = 1 - R_{ct(1)} / R_{ct(2)} \times 100$$

where R<sub>ct(1)</sub> and R<sub>ct(2)</sub> are the charge transfer resistances in the HCl solution in the absence and in the presence of the inhibitors, respectively. IE (%) values increased with increasing inhibitor concentration. The values of the electrochemical parameters derived from Nyquist plots for steel corrosion in the absence and presence of silica and silica/polyacrylamide nanocomposite with

different concentrations are given in Tables 1 and 2, respectively. It can be seen from Tables 1 and 2 that the  $R_{ct}$  values increased with increasing concentrations of the inhibitors. It is clear that the addition of inhibitor increases the adsorption of silica/polyacrylamide nanocomposite over the steel surface and results in the formation of a protective layer, which may decrease the charge transfer between the steel surface and the corrosive medium [45]. A high charge-transfer resistance is associated with a slower corroding system. The decrease in  $C_{dl}$  values, which normally results from a decrease in the dielectric constant and/or an increase in the double-layer thickness. This suggests that these nanocomposites act via adsorption at the steel/solution interface [46], thereby protecting the steel from corrosive attack [47-48]. The maximum inhibitive effect and the highest charge transfer resistance have been found for silica/polyacrylamide nanocomposite, which exhibited higher film resistance than that of silica alone. The results can be attributed to more and rapid adsorption of silica/polyacrylamide nanocomposite and accompanied by a formation of a protective layer, which shielded the reactive steel surface from the aggressive acid environment.

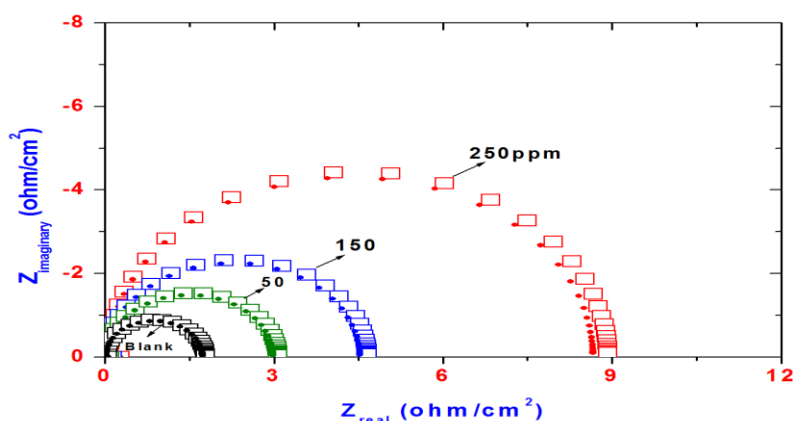


**Figure 5.** Nyquist plot for steel for steel in 1m HCl solution containing different concentrations of silica.

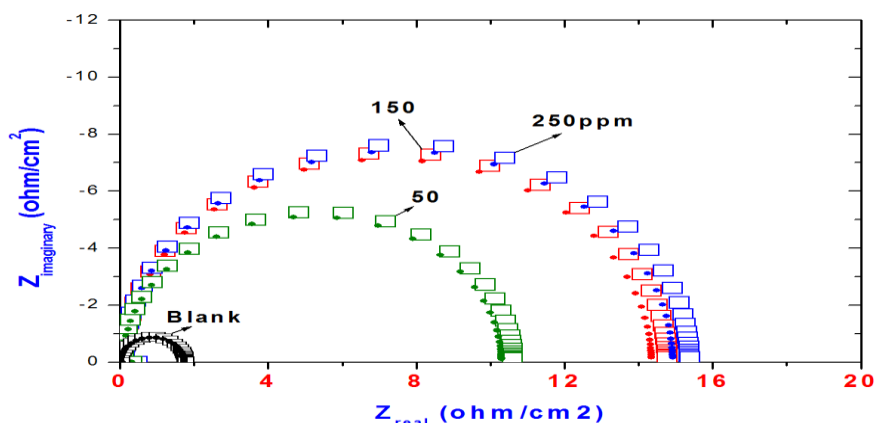


**Figure 6.** Nyquist plot for steel for steel in 1m HCl solution containing different concentrations of silica/polyacrylamide nanocomposite.

#### 4. CONCLUSIONS

1. Encapsulation of silica/polyacrylamide composite core/shell was carried out without agglomeration using crosslinking dispersion radical polymerization technique.

2. Silica/polyacrylamide nanocomposite is a good corrosion inhibitor for the steel protection in 1 M HCl solution. The inhibitory efficiency increases with increasing the concentration.

3. Electrochemical results indicated that silica/polyacrylamide nanocomposite act as mixed type inhibitor by getting adsorbed on anodic as well as cathodic sites on the steel surface.

4. All the impedance spectra exhibit one single depressed semicircle, and the diameter of semicircle increases with the increase in inhibitor concentration. The corrosion of steel is mainly controlled by charge transfer process.

#### ACKNOWLEDGEMENT

The project was supported by King Saud University, Deanship of Scientific Research, Research Chair

#### References

1. B. Radhakrishnan, R. Ranjan, W.J. Brittain, *Soft Matter*, 2 (2006) 386–396.
2. R. Atkin, L-M. De Fina, U. Kiederling, G. G. Warr, *J. Phys. Chem. B*, 113 (2009) 12201–12213.
3. Y. He, Z. Li, P. Simone, T. P. Lodge, *J. Am. Chem. Soc.*, 128(2006)2745.
4. F. Caruso, *Adv. Mater.*, 13(2001) 11.
5. E. Bourgeat-Lami, *J. Nanosci. Nanotechnol.*, 2 (2002) 1.
6. E. Bourgeat-Lami, P. Espiard, A. Guyot, *Polymer*, 36 (1995)4385.
7. E. Bourgeat-Lami, M. Insulaire, S. Reculosa, A. Perro, S. Ravaine, E. Duguet, *J. Nanosci. Nanotechnol.*, 6 (2006) 432.
8. Z. Zeng, J. Yu, Z. X. Guo, *Macromol. Chem. Phys.*, 205(2004)2197.
9. C. Graf, D. L. J. Vossen, A. Imhof, A. van Blaaderen, *Langmuir* 2003, 19, 6693.
10. Y. Lu, J. McLellan, Y. N. Xia, *Langmuir* 20 (2004) 3464.
11. S. W. Zhang, S. X. Zhou, Y. M. Weng, L. M. Wu, *Langmuir*, 22 (2006) 4679.
12. L. L. Becroft, C. K. Ober, *Chem. Mater.*, 9 (1997) 1302.
13. Y. Kojima, A. A. Usuki, M. Kawasumi, A. Okada, T. Kurauchi, O. Kamigaito, *J. Polym. Sci., Part A: Polym. Chem.*, 31 (1993) 983.
14. Y. Kojima, A. Usuki, M. Kuwasumi, A. Okada, Y. Fukushima, T. Kurauchi, O. Kamigaito, *J. Mater. Res.*, 8(1993)1185.
15. A. K. Gaharwar, P.J. Schexnailder, Q. Jin, C-J. Wu, G. Schmidt, *Applied Materials & interfaces.*, 2(2010) 3119–3127.
16. L.M. Palomino, P.H. Suegama, I.V. Aoki, M.F. Montemor, H.G. De Melo, *Corros. Sci.*, 50 (2008) 1258.
17. H. Wang, R. Akid, *Corros. Sci.* 50 (2008) 1142.
18. W. Trabelsi, P. Cecilio, M.G.S. Ferreira, K. Yasakau, M.L. Zheludkevich, M.F. Montemor, *Prog. Org. Coat.*, 59 (2007) 214
19. Y. Castro, A. Duran, J.J. Damborenea, A. Conde, *Electrochim. Acta* 53 (2008) 6008.
20. A. Phanasaonkar, V.S. Raja, *Surface & Coatings Technology*, 203 (2009) 2260–2271.
21. M. Quinet, B. Neveu, V. Moutarlier, P. Audebert, L. Ricq, *Prog. Org. Coat.* 58 (2007) 46.
22. M.F. Montemor, A.M. Cabral, M.L. Zheludkevich, M.G. Ferreira, *Surf. Coat. Technol.* 200 (2006) 2875.

23. V. Palanivel, D. Zhu, W.J. Van Ooij, *Prog. Org. Coat.* 47 (2003) 384.
24. A.J. Paine, *Macromolecules*, 23 (1990) 3109.
25. Q. Lan, F. Yang, S. Zhang, S. Liu, J. Xu, D. Sun, *Colloids and Surfaces A: Physicochem Eng Aspects*, 302 (2007) 126.
26. Q. Qu, Z. Hao, L. Li, W. Bai, Z. Ding, *Corros. Sci.* 51 (2009) 569.
27. F. Bentiss, M. Lebrini, M. Lagrenée, *Corros. Sci.* 47 (2005) 2915.
28. Q. Qu, S. Jiang, W. Bai, L. Li, *Electrochim. Acta* 52 (2007) 6811.
29. C.M. Goulart, A. Esteves-Souza, C.A. Martinez-Huitle, C.J.F. Rodrigues, M.A.M. Maciel, A. Echevarria, *Corros. Sci.* 67 (2013) 281.
30. K.F. Khaled, N. Jackerman, *Electrochim. Acta* 48 (2003) 2715.
31. I. Ahamad, M.A. Quraishi, *Corros. Sci.* 51 (2009) 2006.
32. M.A. Hegazy, A.M. Badawi, S.S. Abd El Rehim, W.M. Kamel, *Corros. Sci.* 69 (2013) 110.
33. Q.B. Zhang, Y.X. Hua, *Electrochim. Acta* 54 (2009) 1881.
34. F. Touhami, A. Aouniti, Y. Abed, B. Hammouti, S. Kertit, A. Ramdani, K. Elkacemi, *Corros. Sci.* 42 (2000) 929.
35. M. El Achouri, S. Kertit, H.M. Gouytaya, B. Nciri, Y. Bensouda, L. Perez, M.R. Infante, K. Elkacemi, *Prog. Org. Coat.* 43 (2001) 267.
36. F. Bentiss, M. Lagrenée, M. Traisnel, J.C. Hornez, *Corros. Sci.* 41 (1999) 789.
37. R. Solmaz, *Corros. Sci.* 79 (2014) 169.
38. F. Zhang, Y. Tang, Z. Cao, W. Jing, Z. Wu, Y. Chen, *Corros. Sci.* 61 (2012) 1.
39. W.H. Mulder, J.H. Sluyters, *Electrochim. Acta* 33 (1988) 303.
40. F.B. Growcock, V.R. Lopp, *Corros. Sci.* 28 (1988) 397.
41. M. Lagren, B. Mernari, N. Chaibi, M. Traisnel, H. Vezin, F. Bentiss *Corros. Sci.* 43 (2001) 951.
42. H. Ashassi-Sorkhabi, B. Shaabani, D. Seifzadeh, *Electrochim. Acta* 50 (2005) 3446.
43. M. Tourabi, K. Nohair, M. Traisnel, C. Jama, F. Bentiss, *Corros. Sci.* 75 (2013) 123.
44. B. Xu, Y. Liu, X. Yin, W. Yang, Y. Chen *Corros. Sci.* 74 (2013) 206.
45. N. Soltani, N. Tavakkoli, M. Khayatkashani, M.R. Jalali, *Corros. Sci.* 62 (2012) 122.
46. S. Nofrizal, A.A. Rahim, B. Saad, P.B. Raja, A.M. Shah, S. Yahya, *Metal. Mate. Trans. A* 43 (2012) 1382.
47. X. Li, S. Deng, H. Fu, *Corros. Sci.* 55 (2012) 280.
48. E.E. Oguzie, C.B. Adindu, C.K. Enenebeaku, C.E. Ogukwe, M.A. Chidiebere, K.L. Oguzie, *J. Phys. Chem. C* 116 (2012) 13603